

Quantum effects on the evaporation of PBHs: contributions to dark matter

Md Riajul Haque^{1a}, Suvashis Maity^{1b}, Debaprasad Maity^{2c}, Yann Mambrini^{3d},

¹Centre for Strings, Gravitation and Cosmology, Department of Physics, Indian Institute of Technology Madras, Chennai 600036, India

²Department of Physics, Indian Institute of Technology Guwahati, Guwahati, Assam, India

³ Université Paris-Saclay, CNRS/IN2P3, IJCLab, 91405 Orsay, France

E-mail: a.riaj.0009@gmail.com, b.suvashis@physics.iitm.ac.in, c.debu@iitg.ac.in,
d.yann.mambrini@ijclab.in2p3.fr

Abstract. We compute the relic abundance of dark matter in the presence of Primordial Black Holes (PBHs) beyond the semiclassical approximation. We take into account the quantum corrections due to the memory burden effect, which is assumed to suppress the black hole evaporation rate by the inverse power of its own entropy. Such quantum effect significantly enhances the lifetime, rendering the possibility of PBH mass $\lesssim 10^9$ g being the sole dark matter (DM) candidate. However, Nature can not rule out the existence of fundamental particles such as DM. We, therefore, include the possibility of populating the dark sector by the decay of PBHs to those fundamental particles, adding the contribution to stable PBH whose lifetime is extended due to the quantum corrections. Depending on the strength of the burden effect, we show that a wide range of parameter space opens up in the initial PBH mass and fundamental dark matter mass plane that respects the correct relic abundance.

Contents

1	Introduction	1
2	Mass evolution of PBHs due to evaporation and the effects of memory burden	2
3	Production of dark matter and the effects of memory burden	7
3.1	Number of dark matter particles emitted from the evaporation of a PBH	7
3.2	Dark matter from the evaporation of PBHs before BBN	9
3.2.1	Computation of β_c	9
3.2.2	$\beta > \beta_c$	11
3.2.3	$\beta < \beta_c$	13
3.3	Dark matter from the stable PBHs with Hawking evaporation (<i>phase-I</i>) before BBN	14
4	Conclusions	18

1 Introduction

Primordial Black holes (PBHs) are fascinating objects proposed more than 50 years ago [1], but they have recently gained widespread interest, particularly in the context of dark matter (DM) [2–11] and searches for gravitational waves [12–19]. Indeed, contrary to the conventional DM matter candidates, the proposal of PBHs as a possible relic could be considered a huge conceptual jump, which does not require any new physics beyond the Standard Model and gravity. However, black holes are metastable candidates and emit fundamental particles through the well-known phenomena of Hawking radiation [20, 21]. In vanilla scenarios, PBHs weighing less than 10^{15} grams have already evaporated, so they cannot be considered as potential dark matter candidates, even if they can still play an important role in reheating [22], leptogenesis [23–25], gravitational wave [26–33] or dark matter production [34–37]. In fact, even PBHs of higher masses, in spite of having survived, enter in conflict with observations of γ -ray [38–40], light elements abundance during big bang nucleosynthesis (BBN) [41, 42] or other indirect observations [43–47]. Therefore, the idea of PBHs being a real DM candidate is gradually fading away except within a very narrow mass window $10^{16} - 10^{23}$ grams (see the review [48] and references therein for a complete analysis).

However, this semiclassical phenomenon of black hole radiation heavily relies on the assumption that during the evaporation process, the black hole remains classical till the end of its lifetime. Over the years, it has been realized that such a semiclassical approach should not remain self-similar [49] throughout its entire lifetime, and new physics should come into play, particularly in the parlance of the information loss paradox. It has recently been argued [50] that during its evaporation, when the mass of a BH reaches a certain fraction of its initial value, the backreaction can not be ignored, and it can potentially reduce the evaporation rate by the inverse power law of its entropy S^{-k} . This, in turn, significantly enhances the lifetime of black holes, reopening the possibility of the BHs of mass $< 10^{15}$ grams being the sole DM candidate as recently discussed in [51, 52]. In this paper, we will be inclusive, considering also the possibility of a multi-component scenario, where part of the total DM

could be fundamental particles produced through the evaporation process. Such inclusion and its implicit dependence on the enhanced BHs lifetime are, therefore, expected to alter the existing constraints [42, 48] on particle DM and PBH parameter space significantly, which is the subject of our study.

At this point, we shall mention that there are several potential mechanisms through which PBHs can form. The mechanism includes the collapse of the enhanced density perturbations that originated during inflation [15, 19, 53–57], bubble collisions [58], collapse of domain walls [59, 60], collapse of cosmic strings [61, 62], electroweak phase transition [63], first-order phase transitions [64, 65], and formation of other topological defects [66, 67]. In this work, we will not focus on the details of how the PBHs are formed. Rather, our discussion spans around the evolution, especially the evaporation of the PBHs and the effects of memory burden on the process.

The paper is organized as follows. In section 2, we discuss the evolution of PBH mass when the memory effect is active after a certain fraction of the initial mass of the PBH remains due to Hawking evaporation. In section 3, we analyze the effects of the memory burden on the DM that is produced due to the evaporation of PBHs. We shall distinguish two different scenarios in this context. In section 3.2, we consider the mass range of PBHs that evaporates *before* BBN completely, whereas in section 3.3, we look at the case where the initial phase of evaporation happens before BBN while the PBHs are *stable* till present day. We then conclude in section 4.

Before we begin, let us list out the main notations that we will be using throughout our analysis:

Notations about scale factor and time

$a_{\text{in}}, t_{\text{in}}$: Scale factor and time at the PBH formation

$a_{\text{q}}, t_{\text{q}}$: Scale factor and time at the onset of memory burden

$a_{\text{BH}}, t_{\text{BH}}$: Scale factor and time at PBH domination

$a_{\text{ev}}, t_{\text{ev}}$: Scale factor and time at the PBH evaporation

$a_{\text{BBN}}, t_{\text{BBN}}$: Scale factor and time at BBN

2 Mass evolution of PBHs due to evaporation and the effects of memory burden

As a first step, we need to study the evaporation process of the black hole in detail, taking into account the memory burden effects (for a detailed discussion see Refs. [50–52]). After the formation, PBH energy density $\rho_{\text{BH}} = n_{\text{BH}} M_{\text{BH}}$ is mostly governed by two quantities: the PBH number density, n_{BH} which decreases as the universe expands as $n_{\text{BH}} \sim a^{-3}$ (a be the scale factor), and the mass of PBHs M_{BH} , which changes due to the mechanisms of evaporation and accretion. We shall first present a brief summary of the evaporation process in the semiclassical approximation before considering the quantum effect. The Hawking temperature, T_{BH} and entropy, S associated with a PBH with mass M_{BH} are given by

$$T_{\text{BH}} = \frac{M_P^2}{M_{\text{BH}}}, \quad S = \frac{1}{2} \left(\frac{M_{\text{BH}}}{M_P} \right)^2 = \frac{1}{2} \left(\frac{M_P}{T_{\text{BH}}} \right)^2, \quad (2.1)$$

where $M_P = 1/\sqrt{8\pi G_N} \simeq 2.4 \times 10^{18}$ GeV is the reduced Planck mass. If we consider that the evaporation happens by purely Hawking radiation then the rate of change of mass at any point is [20]

$$\frac{dM_{\text{BH}}}{dt} = -\epsilon \frac{M_P^4}{M_{\text{BH}}^2}, \quad (2.2)$$

where $\epsilon = \frac{27}{4} \frac{\pi g_*(T_{\text{BH}})}{480}$, with $g_*(T_{\text{BH}})$ being the number of degrees of freedom associated with the PBH temperature. The factor $27/4$ accounts for the graybody factor¹ [70], and the negative sign on the right-hand side is since the PBH mass decreases with time due to the evaporation. We shall note that the accretion effect is negligible here.

After integrating Eq. (2.2) from the time of the formation of PBH, t_{in} to the time t , we find the PBH mass at t is given by

$$M_{\text{BH}}(t) = M_{\text{in}} [1 - \Gamma_{\text{BH}}^0 (t - t_{\text{in}})]^{1/3}, \quad (2.3)$$

where M_{in} is the initial mass of the PBH, which is related to the horizon size at the time of formation,

$$M_{\text{in}} = \frac{4}{3} \pi \gamma \rho_{\text{in}} H_{\text{in}}^{-3} = 4\pi \gamma M_P^2 / H_{\text{in}}, \quad (2.4)$$

where we assume the formation of PBHs in a radiation-dominated universe, so $H_{\text{in}}^2 = \rho_R(a_{\text{in}})/(3M_P^2)$, and $\rho_R(a_{\text{in}})$ is the background radiation energy density and can be connected with the formation temperature T_{in} , $\rho_R(a_{\text{in}}) = \alpha T_{\text{in}}^4$ with $\alpha = \pi^2 g_*/30$. Here, g_* is the relativistic degrees of freedom associated with the thermal bath, which we assume $g_* = 106.75$. In Eq. (2.4), γ represents the efficiency factor for collapse, which defines what fraction of the total mass inside the Hubble radius collapses to form PBHs. For standard radiation domination, $\gamma \sim 0.2$ [1]. The time of the PBH formation can be related to the formation mass of the PBH as $t_{\text{in}} = M_{\text{in}}/(8\pi \gamma M_P^2)$, where we have considered a radiation-dominated Universe, $H(t) = 1/(2t)$. The quantity $\Gamma_{\text{BH}}^0 = 3\epsilon M_P^4/M_{\text{in}}^3$ is the decay width associated with the evaporation of PBH. Note that the evolution of the PBH mass described by Eq. (2.3) is really abrupt, hence Stephen Hawking's own description of it as an 'explosion'. The mass of the PBH $M_{\text{BH}}(t)$ remains almost constant $M_{\text{BH}} \sim M_{\text{in}}$ during the whole process of evaporation, and then the PBH rapidly decays at $t = t_{\text{ev}}$.

We find the lifetime, t_{ev} of the PBH by solving $M_{\text{BH}}(t_{\text{ev}}) = 0$ in Eq. (2.3)

$$t_{\text{ev}} = \frac{1}{\Gamma_{\text{BH}}^0} = \frac{M_{\text{in}}^3}{3\epsilon M_P^4} \simeq 2.4 \times 10^{-28} \left(\frac{M_{\text{in}}}{1 \text{ g}} \right)^3 \text{ s}, \quad (2.5)$$

where we supposed $t_{\text{ev}} \gg t_{\text{in}}$. During radiation domination, the Hubble parameter is related to the radiation temperature as $H = \sqrt{\frac{\alpha}{3}} \frac{T^2}{M_P}$. One can then connect time and temperature during the radiation era as

$$t = \frac{1}{2} \sqrt{\frac{3}{\alpha}} \frac{M_P}{T^2}. \quad (2.6)$$

From Eq. (2.5), we recover that PBHs of mass $\gtrsim 10^{15}$ grams should not have decayed yet, whereas PBHs of mass below $\lesssim 10^9$ grams should have decayed before the BBN epoch, or equivalently, before 1 second².

¹For instance, a more thorough formulation for the greybody factor can be found in Refs. [34, 68, 69].

²Note that all the above conclusions are under the assumption that the PBHs radiate particles in a self-similar semiclassical process until their end of life.

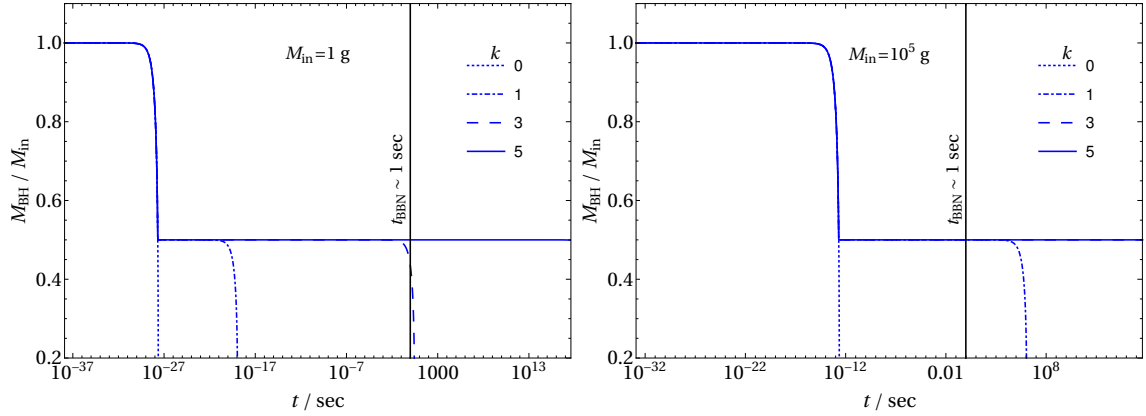


Figure 1. Evolution of the mass of the PBH as a function of time for different values of k are plotted here. In the left plot, we have chosen $M_{\text{in}} = 1 \text{ g}$, and in the right plot, we have chosen $M_{\text{in}} = 10^5 \text{ g}$ and q is set to the value $q = 1/2$. We have chosen four values of k , where $k = 0, 1, 3$, and 5 are plotted in dotted, dot-dashed, dashed, and solid lines, respectively. We have taken the maximum value of time to be the current age of the universe, $t \sim 4 \times 10^{17} \text{ sec}$. We see the lifetime of a PBH increases with k .

We now consider a special type of correction to the evaporation process proposed in [50]. Such correction is called the memory burden's effect, which essentially suggests that the quantum modes associated with the entropic degrees of freedom of a black hole necessarily have a strong backreaction effect on its own evaporation process. Therefore, the initial semiclassical Hawking evaporation will no longer be valid after a certain time scale. For the purpose of our analysis, we can suppose that the semiclassical regime is valid until the mass of the PBH reaches a certain value, i.e. $M_{\text{BH}} = qM_{\text{in}}$, with $0 < q < 1$. The authors of [51, 52] proposed that the quantum effects begin to be important when $M_{\text{BH}} = (1/2)M_{\text{in}}$, or $q = 1/2$. However, such value is subjected to the detailed quantum mechanical modeling of a black hole. To keep our study as general as possible, let t_q be the time at the end of the semiclassical phase. Then, from Eq. (2.3) we obtain

$$t_q = \frac{1 - q^3}{\Gamma_{\text{BH}}^0}, \quad (2.7)$$

where Γ_{BH}^0 is defined before. In the above equation, with the substitution of $q = 0$, one shall recover the full evaporation time, t_{ev} . Once the mass of the PBH reaches qM_{in} , at t_q , the quantum memory effect starts dominating. Upon parameterizing the memory burden effect in the second phase, the evolution of the mass which is given in Eq. (2.2) modifies to³

$$\frac{dM_{\text{BH}}}{dt} = -\frac{\epsilon}{[S(M_{\text{BH}})]^k} \frac{M_P^4}{M_{\text{BH}}^2}, \quad (2.8)$$

where $S(M_{\text{BH}})$ is the BH entropy defined in Eq. (2.1). The parameter k characterizes the efficiency of the backreaction effect. So far, we do not have any theoretical constraints on the value of the power k except for its probably being a positive number. For our present purpose, we would take it to be an integer. We can understand the quantum effect as a slowdown of

³Note that M_{BH} being almost constant during the evaporation process, $S(M_{\text{BH}}) \sim S(M_{\text{in}})$, which corresponds to the approximation made in [52], and which we will apply for our numerical analysis.

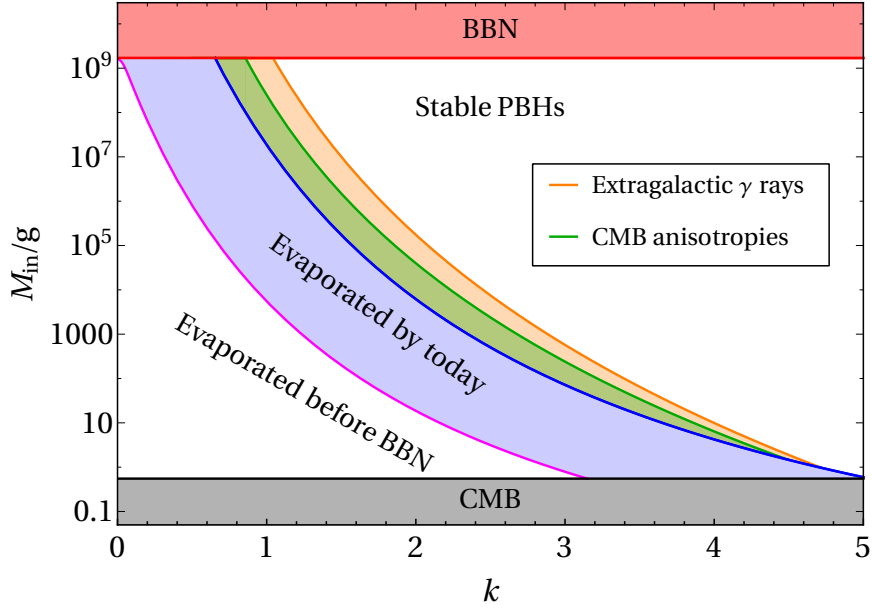


Figure 2. Different limits on the formation mass as a function of k are plotted here. The red line represents the M_{in} above which the half-life of PBH will be after BBN. The region above the blue line represents M_{in} for the stable PBHs today. The region below the magenta line represents M_{in} for the PBHs that evaporated before BBN. The black line corresponds to the minimum allowed value of the formation mass, M_{in} calculated from the maximum allowed value of the inflationary energy scale $H_{\text{inf}} \sim 5 \times 10^{13}$ GeV, set by the upper bound of the tensor-to-scalar ratio $r < 0.036$ from CMB data [71]. The orange and the green shaded regions are the constraints from the Extragalactic γ rays and CMB anisotropies, respectively, on stable PBHs where PBHs cannot be total dark matter relic observed today, which indicates $f_{\text{PBH}} < 1$, f_{PBH} being the ratio between the PBH and the dark matter energy density calculated today (see the text for details). For the restriction from Extragalactic γ rays and CMB anisotropies, we use Ref. [52].

the decay due to an excess of entropy, produced by its evaporation, surrounding the PBH. After integrating Eq. (2.8) we obtain

$$M_{\text{BH}} = qM_{\text{in}} \left[1 - \Gamma_{\text{BH}}^k (t - t_q) \right]^{\frac{1}{3+2k}}, \quad \text{with} \quad \Gamma_{\text{BH}}^k = 2^k (3 + 2k) \epsilon M_P \left(\frac{M_P}{qM_{\text{in}}} \right)^{3+2k}. \quad (2.9)$$

From Eq. (2.9), we obtain that the second phase of evaporation will occur for a time $\sim 1/\Gamma_{\text{BH}}^k$. Hence, the total evaporation time is given by $t_{\text{ev}}^k = t_q + 1/\Gamma_{\text{BH}}^k \simeq 1/\Gamma_{\text{BH}}^k$. It is straightforward to see that for $k = 0$ and $q = 1$, t_{ev}^k will be equal to as given in Eq. (2.5). Also for $k > 0$, we have $t_{\text{ev}}^k \gg t_{\text{ev}}$ (for a detailed discussion see Ref. [51]) and we obtain

$$t_{\text{ev}}^k \simeq \frac{q^{3+2k}}{2^k (3 + 2k)} \left(\frac{M_{\text{in}}}{4.3 \times 10^{-6} \text{ g}} \right)^{3+2k} 5.7 \times 10^{-44} \text{ s}, \quad (2.10)$$

which gives, for instance, for $k = 1$ and $q = 1/2$

$$t_{\text{ev}}^{k=1} \simeq 1.2 \times 10^{-19} \left(\frac{M_{\text{in}}}{1 \text{ g}} \right)^5 \text{ s} \simeq 4 \times 10^{17} \left(\frac{M_{\text{in}}}{2 \times 10^7 \text{ g}} \right)^5 \text{ s}. \quad (2.11)$$

We then conclude that even in the minimal $k = 1$ case, a PBH of only 2×10^7 grams can survive until the present time and contribute to the DM relic abundance. To illustrate our

M_{in} (g)	t_{in} (sec)	$t_{\text{ev}}^{k=0}$ (sec)	$t_{\text{ev}}^{k=1}$ (sec)	$t_{\text{ev}}^{k=3}$ (sec)	$t_{\text{ev}}^{k=5}$ (sec)
1	1.24×10^{-38}	2.34×10^{-28}	1.95×10^{-19}	8.63	3.82×10^{20}
10^4	1.24×10^{-34}	2.34×10^{-16}	19.489	8.63×10^{36}	3.82×10^{72}
10^8	1.24×10^{-30}	2.3×10^{-4}	1.94×10^{21}	8.63×10^{72}	3.82×10^{124}

Table 1. The time of formation and evaporation for different M_{in} are tabulated here. $k = 0$ represents the case of pure Hawking radiation.

result, we show in the left panel of Fig. 1 the evolution of PBH mass as a function of time for $q = 1/2$ and different values of $k = 0, 1, 3$ and 5 , which are plotted in dotted, dot-dashed, dashed and solid lines respectively. Obviously, we see that for $k = 0$, there is no second phase of evolution because the treatment is completely semiclassical. As the value of k increases, the greater is the quantum effect, slowing down the process of decay even further. We also presents some numerical results of the evaporation time t_{ev} in Table 1 for 3 PBHs masses ($1, 10^4$ and 10^8 g) with and without taking into account the memory burden effect for different values of k , and with the formation time t_{in} for information.

We focus on the case where the semiclassical phase of the evaporation ends before BBN. The maximum initial mass of a PBH for which it will half evaporate before BBN can be obtained from Eq. (2.7) with $q = 1/2$. This is independent of the value of k and is represented by the red line on top of the right panel in Fig. 1. The red-shaded region above the line indicates the region where the Hawking evaporation of PBHs happens after BBN, i.e., $t_q > t_{\text{BBN}}$. Note that we assume $t_{\text{BBN}} = 1$ second throughout our analysis. On the other hand, the magenta line corresponds to the maximum value of M_{in} for which the complete evaporation happens before BBN, i.e., $t_{\text{ev}}^{\text{tot}} \leq t_{\text{BBN}}$ and the value is given by

$$M_{\text{in}} = \frac{M_P}{q} \left((3 + 2k) \epsilon 2^k t_{\text{BBN}} M_P \right)^{1/(2k+3)}. \quad (2.12)$$

We see that with the increase in the value of k , the PBHs become more stable hence the maximum value of M_{in} that evaporates before BBN decreases.

However, the interesting situation is when PBHs' lifetime in the semiclassical approximation is *below* the BBN limit (below the red line) while the quantum effect renders them stable at the scale of the age of the Universe. This region appears to be above the blue line in Fig. 1. In other words, considering the quantum effect, some of the PBHs with mass $M_{\text{in}} \leq 10^8$ g will survive till today. For instance, for $k = 1, 2$ and 3 the lower limit of the mass that should have survived are $\sim 2 \times 10^7$ g, 7×10^3 g, and 80 g respectively. However, being stable at the scale of the age of the Universe is not sufficient. Indeed, the metastability of PBHs implies the possibility to observe them through their radiation in the CMB or extragalactic γ -ray. The non-observation of such signals exclude part of the region, shaded in green and orange of Fig. 2 respectively, to be the sole DM candidate. Therefore, if at all PBHs form in those mass ranges, their fractional abundance must be very small, and an additional component needs to be incorporated to match the present DM abundance, under the form of dark particles, for instance. We will calculate in detail those contributions of additional particles like DM components produced directly from the PBHs decay.

To be more precise, PBHs can act as DM due to their cold, non-interacting nature. The fraction of total DM that is given by the stable PBHs today is often referred to as

f_{PBH} . In Fig. 2, the region above the blue line has two additional constraints on f_{PBH} coming from extragalactic γ rays and from CMB anisotropies which are shaded in orange and green, respectively. PBHs can not contribute to the total dark matter in these regions, i.e., $f_{\text{PBH}} < 1$. The contribution to the extragalactic γ rays comes from the evaporation of PBHs between the time of recombination and the present time. On the other hand, the evaporation of PBHs can inject energy into the neutral medium and ionize it after the recombination. This restricts the amount of f_{PBH} as the injected energy affects the angular power spectrum of temperature and polarization of CMB due to the rescattering of CMB photons. A detailed discussion about these constraints can be found in Ref. [52].

As emphasized earlier, in this paper, we consider the present-day DM to be composed of both PBHs and fundamental particles. Our work will then focus on these two interesting regions, the unshaded ones in Fig. 2, where dark matter can be produced by PBH evaporation while not being excluded by other constraints. Indeed, whereas PBHs can be dark matter candidates within this parameter space, the fact that the semiclassical process takes place before BBN also creates the possibility of producing a particle-like dark matter candidate through the PBH's early decay. In that case, the relic abundance should be the sum of the PBH dark decay product and the surviving PBH density. Note that the black line corresponds to the minimum value of M_{in} set by the maximum allowed value of the inflationary energy scale $H_{\text{inf}} \sim 5 \times 10^{13}$ GeV, calculated considering the upper bound of the tensor-to scalar ratio $r < 0.036$ from Planck together with latest BICEP/Keck data [71, 72].

3 Production of dark matter and the effects of memory burden

To study the effects of the memory burden on the production of dark matter from the evaporation of PBHs, we should consider two possible scenarios. We shall first consider the case when the PBHs evaporate completely before BBN, and the dark matter generated from the evaporation satisfy the present dark matter relic. This is represented by the white region below the magenta line in Fig. 2. Another possibility is to consider that the first phase of Hawking evaporation (semiclassical approximation) happens *before* the BBN, whereas the PBH remains stable till today due to the memory effect. This is the white region above the blue line of Fig. 2. First, we need to compute the number of particles that are emitted from the evaporation of one PBH. Note that from now on, we will coin *phase-I* the semiclassical evaporation phase, and *phase-II* the second phase, where quantum correction is effective.

3.1 Number of dark matter particles emitted from the evaporation of a PBH

Let N_j be the number of particles that are emitted from the evaporation of one PBH. We divide N_j into two parts N_{1j} and N_{2j} , which are the number of particles emitted from PBHs for *phase-I* and *phase-II*, respectively. We shall mention that BH mass and spin affect the production rate of any species that is generated from evaporation. In this work, for simplicity, we restrict ourselves to the case of spin-zero Schwarzschild BH. The emission rate of particles j with mass m_j and internal degrees of freedom g_j that escape the horizon of radius R_S per unit time per unit energy interval due to the Hawking radiation in the *phase-I* is given by [22, 35]

$$\frac{d^2 N_{1j}}{dE dt} = \frac{27}{4} \pi R_S^2 \frac{g_j}{2\pi^2} \frac{E^2}{\exp(E/T_{\text{BH}}) \pm 1} = \frac{27}{4} \frac{g_j}{32\pi^3} \frac{(E/T_{\text{BH}})^2}{\exp(E/T_{\text{BH}}) \pm 1} \quad (3.1)$$

where the Schwarzschild radius is given by $R_S = M_{\text{BH}}/(4\pi M_P^2)$. The sign \pm is used for fermionic and bosonic particles, respectively. We can estimate the total energy emitted per unit time from a BH by integrating over Eq. (3.1) as

$$\frac{dN_{1j}}{dt} = \frac{27}{4} \frac{\xi g_j \zeta(3)}{16\pi^3} \frac{M_P^2}{M_{\text{BH}}}, \quad \text{where } \xi = \begin{cases} 1 & \text{for bosons} \\ \frac{3}{4} & \text{for fermions} \end{cases}. \quad (3.2)$$

In the *phase-II*, the emission rate is reduced, affected by the quantum corrections :

$$\frac{d^2 N_{2j}}{dE dt} = \frac{1}{[S(M_{\text{BH}})]^k} \frac{d^2 N_{1j}}{dE dt}, \quad (3.3)$$

where the expression for $d^2 N_{1j}/(dE dt)$ is given in Eq. (3.1). After integrating over all the energy modes, the emission rate is given by

$$\frac{dN_{2j}}{dt} = \frac{27}{4} \frac{\xi g_j \zeta(3) 2^k}{16\pi^3} \frac{M_P^{2+2k}}{M_{\text{BH}}^{1+2k}}. \quad (3.4)$$

The total number of particles emitted from the evaporation of a BH can be obtained by integrating Eq. (3.2) and Eq. (3.4). Depending on the mass of the emitted particle relative to the PBH formation temperature $T_{\text{BH}}^{\text{in}}$, one should distinguish two cases. If $m_j < T_{\text{BH}}^{\text{in}}$, the production of particles happen throughout the lifetime of the PBH, i.e., from the initial time t_{in} to a final time t_{ev} . Indeed, the BH temperature *increasing* with time, the relation $m_j < T_{\text{BH}}$ will always hold. On the other hand, if $m_j > T_{\text{BH}}^{\text{in}}$, the evaporation will start from a time t_j where $m_j = T_{\text{BH}}(t_j)$, the production being exponentially suppressed before. This can happen either during *phase-I* ($t_j < t_q$) or during *phase-II* ($t_j > t_q$). Combining Eq. (2.3) and Eq. (2.9) we can calculate the value of t_j

$$t_j = \begin{cases} t_{\text{ev}}^0 \left[1 - \frac{M_P^6}{M_{\text{in}}^3 m_j^3} \right] & \text{for } t_j < t_q \\ t_{\text{ev}}^k \left[1 - \left(\frac{M_P^2}{q M_{\text{in}} m_j} \right)^{3+2k} \right] & \text{for } t_j > t_q, \end{cases} \quad (3.5)$$

where t_q is given by Eq. (2.7) and we supposed $t_j \gg t_{\text{in}}$.

With the relations in hand let us proceed to calculate the number of particle emitted from the evaporation. First we shall consider the case when $m_j < T_{\text{BH}}^{\text{in}}$. To calculate the number in the first phase, we integrate Eq. (3.2) within the limit $[t_{\text{in}}, t_q]$ which leads to

$$N_{1j} = \frac{15\xi g_j \zeta(3)(1-q^2)}{g_*(T_{\text{BH}})\pi^4} \frac{M_{\text{in}}^2}{M_P^2}, \quad (3.6)$$

where we see the case of complete evaporation due to only Hawking radiation can be obtained by substituting $q = 0$. During the second phase of evaporation, we shall integrate Eq. (3.4) from t_q to a final time t , and the number of dark matter emitted is given by

$$N_{2j} = \frac{15\xi g_j \zeta(3)}{g_*(T_{\text{BH}})\pi^4} \frac{q^2 M_{\text{in}}^2}{M_P^2} \left[1 - \left(1 - \frac{t - t_q}{t_{\text{ev}}} \right)^{\frac{2}{3+2k}} \right]. \quad (3.7)$$

The total number of dark matter particles from the evaporation of a PBH can be obtained by adding N_{1j} and N_{2j} from Eq. (3.6) and Eq. (3.7). For those BHs evaporated by today, $t = t_{\text{ev}} \gg t_q$ and we have the total numbers of DM particles emitted from a single BH

$$N_j = N_{1j} + N_{2j} = \frac{15\xi g_j \zeta(3)}{g_*(T_{\text{BH}})\pi^4} \frac{M_{\text{in}}^2}{M_P^2}, \quad (3.8)$$

which is the same as the total number of particles emitted from the Hawking evaporation. This is not surprising as the total number of emitted particles due to the evaporation of a PBH does not depend on the evaporation process.

For the case $m_j > T_{\text{BH}}^{\text{in}}$, we have two different scenarios: $t_j < t_q$ and $t_j > t_q$. For $t_j < t_q$, we get the number of particles emitted during *phase-I* by simply integrating Eq. (3.2) in the interval $[t_j, t_q]$, no particles being produced before due to the Boltzmann suppression factor,

$$N_{1j} = \frac{15\xi g_j \zeta(3)}{g_*(T_{\text{BH}})\pi^4} \left(\frac{M_P^2}{m_j^2} - \frac{q^2 M_{\text{in}}^2}{M_P^2} \right). \quad (3.9)$$

Where we used $M_{\text{BH}}(t_j) = M_P^2/m_j$. The number of particles emitted N_{2j} in the *phase-II* would be the same as obtained in Eq. (3.7). On the other hand, if $t_j > t_q$, corresponding to $m_j > \frac{M_P^2}{qM_{\text{in}}}$, there is obviously no dark matter emission during *phase-I*, i.e., $N_{1j} = 0$. The number of particles emitted during the second phase is given by

$$N_{2j} = \frac{15\xi g_j \zeta(3)}{g_*(T_{\text{BH}})\pi^4} \frac{q^2 M_{\text{in}}^2}{M_P^2} \left[\left(1 - \frac{t_j - t_q}{t_{\text{ev}}} \right)^{\frac{2}{3+2k}} - \left(1 - \frac{t - t_q}{t_{\text{ev}}} \right)^{\frac{2}{3+2k}} \right], \quad (3.10)$$

where we have integrated Eq. (3.4) in the time interval $[t_j, t]$ with t_j given in Eq. (3.5) for $t_j > t_q$. In both cases after complete evaporation, we get the total number of DM particles emitted for $m_j > T_{\text{BH}}^{\text{in}}$ by setting $t = t_{\text{ev}} > t_j \gg t_q$, to be

$$N_j = N_{1j} + N_{2j} = \frac{15\xi g_j \zeta(3)}{g_*(T_{\text{BH}})\pi^4} \frac{M_P^2}{m_j^2}, \quad (3.11)$$

which is again the number of particles emitted by pure Hawking evaporation for $m_j > T_{\text{BH}}^{\text{in}}$ [22, 24, 35]. In the next section, we shall discuss the case where the PBH evaporates completely, before studying the case where relic PBHs could contribute to the dark abundance, in addition to its decay products.

3.2 Dark matter from the evaporation of PBHs before BBN

3.2.1 Computation of β_c

The memory burden effect increases the lifetime of the PBHs. Moreover, increasing the value of k , such burden effect becomes stronger, and as a consequence, it limits the maximum value of the PBH mass that evaporates before BBN, which is also evident from Fig. 2. Note that in this figure, we assume that the memory effect is effective after its half-life ($q = 1/2$). On the other hand, the minimum allowed mass for a PBH is set by the minimum horizon size at the end of inflation, and determined by the energy available of the inflaton. Assuming de-sitter-like inflation and taking the constraint on the tensor-to-scale ratio $r < 0.036$ from Planck combined with the latest BICEP/Keck data [71], the minimum allowed mass is roughly

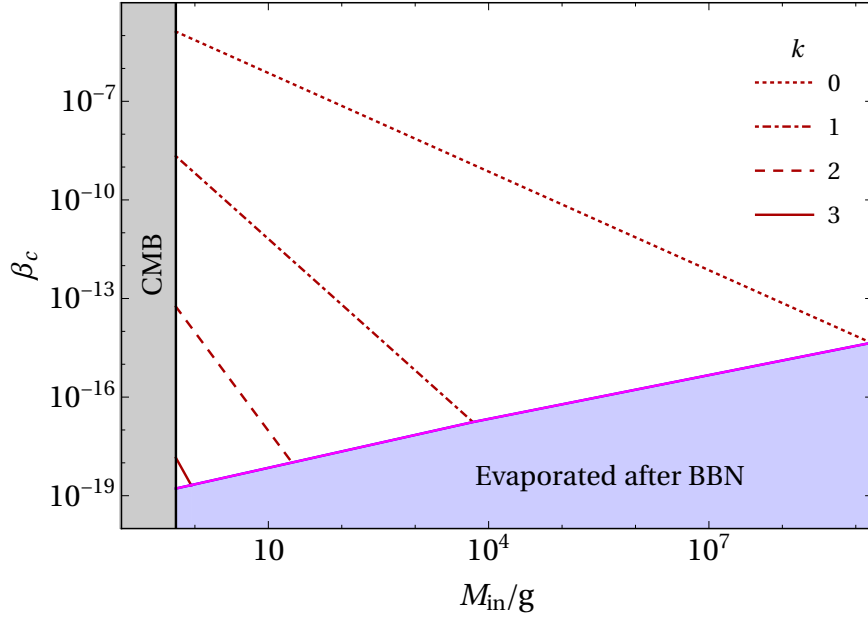


Figure 3. Critical values of beta corresponding to the PBH domination are plotted as a function of M_{in} for different k . We have chosen four values of k where $k = 0, 1, 2$, and 3 are plotted in dotted, dot-dashed, dashed, and solid lines, respectively. The grey-shaded region is excluded from the minimum PBH mass possible, corresponding to the highest energy scale of inflation. The blue-shaded region corresponds to the PBHs that evaporate after BBN.

around $M_{\text{BH}} \gtrsim 0.5$ g. Interestingly, for this minimum PBH mass, one requires $k \lesssim 3$ to ensure it is evaporated completely before BBN.

In this section, we will consider two possible scenarios for dark matter production, depending on the PBH parameters (M_{in}, β) , where $\beta = \rho_{\text{BH}}^{\text{in}}/\rho_R^{\text{in}}$ is the ratio between the PBH energy density over radiation energy density at the point of formation. Initially, we will assume that the radiation energy density always dominates the background. Next, we will suppose that for values of β above a critical value β_c , the PBH energy density dominates over the radiation energy density at some time before the evaporation. In both cases, we shall assume that the dark matter is produced solely from the evaporation of PBHs. Let's first determine β_c .

The radiation energy density evolves as

$$\rho_R(a) = \rho_R^{\text{in}} \left(\frac{a_{\text{in}}}{a} \right)^4, \quad (3.12)$$

where ρ_R^{in} is the radiation energy density at the time of PBH formation, and a_{in} is the corresponding scale factor. We also know that PBHs behave like matter; therefore, the energy density of PBHs varies as $\sim a^{-3}$. At any time, the energy density of PBH can be written in terms of the initial energy density as

$$\rho_{\text{BH}}(a) = \begin{cases} \rho_{\text{BH}}^{\text{in}} \left(\frac{a_{\text{in}}}{a} \right)^3 & \text{for } a < a_q \\ q \rho_{\text{BH}}^{\text{in}} \left(\frac{a_{\text{in}}}{a} \right)^3 & \text{for } a > a_q \end{cases}, \quad (3.13)$$

where for $a \sim a_q$, we assume that the mass of the PBHs will be reduced to qM_{in} instantly. There always exists a β value, i.e., β_c , above which it is possible that after a time t_{BH} , the

PBH energy density dominates over the radiation energy density. Equating Eqs. (3.13) and (3.12), this happens for a scale factor a_{BH}

$$\frac{a_{\text{BH}}}{a_{\text{in}}} = \frac{1}{q\beta}. \quad (3.14)$$

The domination of PBHs is possible if $a_{\text{BH}} < a_{\text{ev}}$, or

$$\beta > \frac{a_{\text{in}}}{qa_{\text{ev}}} = \frac{1}{q} \sqrt{\frac{H_{\text{ev}}}{H_{\text{in}}}} = \frac{1}{q} \sqrt{\frac{\Gamma_{\text{BH}}^k}{2H_{\text{in}}}} = \beta_c, \quad (3.15)$$

or

$$\beta_c = \frac{1}{q^{\frac{5}{2}+k}} \left(\frac{M_P}{M_{\text{in}}} \right)^{1+k} \sqrt{\frac{(3+2k)2^k \epsilon}{8\pi\gamma}}. \quad (3.16)$$

where we used Eqs. (2.4) and (2.9). If one assume $q = 1/2$, we have

$$\beta_c \simeq 5.5 \times 2^{\frac{3k}{2}} \sqrt{(3+2k)} \left(\frac{M_P}{M_{\text{in}}} \right)^{1+k}, \quad (3.17)$$

or

$$\beta_c^{k=0} \simeq 4.0 \times 10^{-5} \left(\frac{1 \text{ g}}{M_{\text{in}}} \right), \quad \beta_c^{k=1} \simeq 6.5 \times 10^{-10} \left(\frac{1 \text{ g}}{M_{\text{in}}} \right)^2, \quad \beta_c^{k=2} \simeq 9.4 \times 10^{-15} \left(\frac{1 \text{ g}}{M_{\text{in}}} \right)^3.$$

As we can notice, the critical value of β , for a given M_{in} , decreases drastically with k . This is understandable because larger k means a longer lifetime. In other words, smaller values of β are necessary to ensure PBH domination. As we increase k , the β_c shifted towards smaller values, such as for $k = 0$ and $M_{\text{in}} = 1 \text{ g}$, $\beta_c \sim 4 \times 10^{-5}$, whereas for $k = 1$, $\beta_c \sim 6 \times 10^{-10}$. We show in Fig. 3 the evolution of β_c as function of M_{in} for different choices of k . Note that even for very light PBHs $\sim 10 \text{ g}$, a value of β as low as 10^{-17} is sufficient for the black holes to dominate the evolution of the Universe before BBN for $k = 2$.

To find the relic abundance of dark matter of the species j today we use [73],

$$\Omega_j h^2 = 1.6 \times 10^8 \frac{g_0}{g_{\text{ev}}} \frac{n_j(a_{\text{ev}})}{T_{\text{ev}}^3} \frac{m_j}{\text{GeV}}, \quad (3.18)$$

where $n_j(a_{\text{ev}})$ is the number density of DM at the end of evaporation, whereas $g_{\text{ev}} \sim 106.75$ and $g_0 = 3.91$ are the effective numbers of light species for entropy at the end of evaporation and present-day, respectively. Once the PBH evaporated, we can write $n_j(a_{\text{ev}}) = N_j n_{\text{BH}}(a_{\text{ev}})$, where N_j be the total number of particles emitted from the evaporation of a single PBH and $n_{\text{BH}}(a_{\text{ev}})$ is the PBH energy density at the point of evaporation. Let us first discuss the case $\beta > \beta_c$.

3.2.2 $\beta > \beta_c$

For $\beta > \beta_c$, there will be a PBH domination *before* PBH decays, which means that the reheating would then be produced entirely through the evaporation. In this case, if one supposes an instant thermalization, the reheating temperature would be the temperature of the decay products given by

$$H^2(a_{\text{ev}}) = \frac{\rho_R(a_{\text{ev}})}{3M_P^2} = \frac{\alpha T_{\text{ev}}^4}{3M_P^2} = \frac{4(\Gamma_{\text{BH}}^k)^2}{9}, \quad (3.19)$$

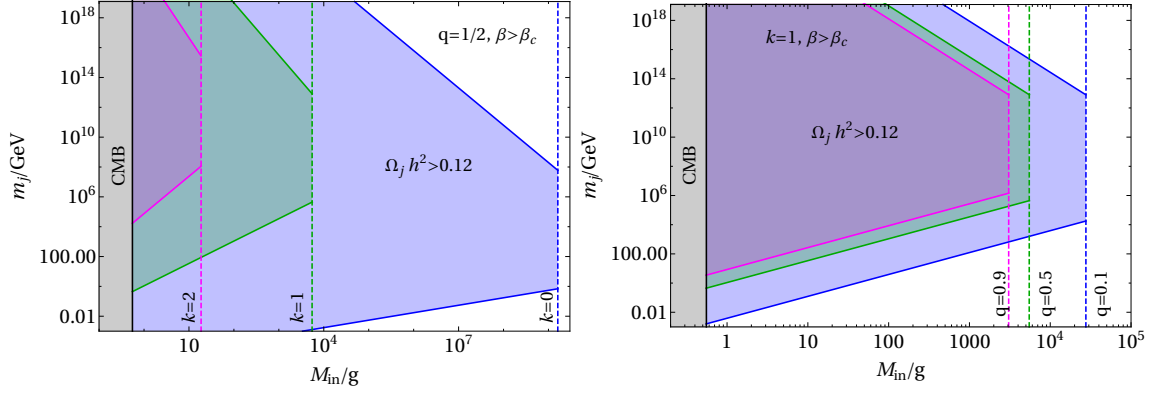


Figure 4. The value of the dark matter mass is plotted here as a function of the formation mass of PBHs for the case where the evaporation happens during PBH domination, i.e., $\beta > \beta_c$. The black lines represent the minimum mass possible for PBHs calculated considering the maximum energy scale of inflation. The shaded regions correspond to dark matter overproduction, $\Omega_j h^2 > 0.12$. The vertical dashed lines represent the maximum M_{in} values allowed to be consistent with the BBN bound. **Left panel:** We have chosen $q = 1/2$ and plotted for three different values of $k = 0, 1$, and 2 , shown in blue, green, and magenta, respectively. **Right panel:** We have chosen $k = 0$ and plotted for three different values of $q = 0.1, 0.5$, and 0.9 , illustrated in blue, green, and magenta, respectively.

$$\Rightarrow T_{\text{ev}} = M_P \left(\frac{4}{3\alpha} \right)^{1/4} \left[(3 + 2k) 2^k \epsilon \left(\frac{M_P}{q M_{\text{in}}} \right)^{3+2k} \right]^{1/2}. \quad (3.20)$$

Since PBH decay happens in a matter-dominated universe, $H(t_{\text{ev}}) = 2/(3t_{\text{ev}})$.

From Eq. (3.19), using $\rho_{\text{BH}}(a_{\text{ev}}) = \rho_R(a_{\text{ev}}) \simeq n_{\text{BH}}(a_{\text{ev}}) \times q M_{\text{in}}$, we have the PBH number density at the evaporation point

$$n_{\text{BH}}(a_{\text{ev}}) = \frac{4}{3} M_P^3 (3 + 2k)^2 2^{2k} \epsilon^2 \left(\frac{M_P}{q M_{\text{in}}} \right)^{7+4k}. \quad (3.21)$$

Combining Eq. (3.18) with Eqs. (3.20) and (3.21), writing $n_j = n_{\text{BH}} \times N_j$, we obtain for $m_j < T_{\text{BH}}^{\text{in}}$

$$\frac{\Omega_j h^2}{0.12} = 2.85 \times 10^6 \frac{\xi g_j}{q^2} \left(2^k (3 + 2k) \right)^{1/2} \left(\frac{M_P}{q M_{\text{in}}} \right)^{\frac{2k+1}{2}} \frac{m_j}{\text{GeV}}. \quad (3.22)$$

Doing the same exercise for $m_j > T_{\text{BH}}^{\text{in}}$, Eq. (3.11) gives

$$\frac{\Omega_j h^2}{0.12} = 1.64 \times 10^{43} \xi g_j \left(2^k (3 + 2k) \right)^{1/2} \left(\frac{M_P}{q M_{\text{in}}} \right)^{\frac{2k+5}{2}} \frac{\text{GeV}}{m_j}. \quad (3.23)$$

We show in Fig. 4 the exclusion parameter due to an overabundance of dark matter in the shaded regions, for different values of k and $q = 1/2$ (on the left) or $k = 1$ and different values of q (on the right). We easily recognize the two allowed regions, for light masses, corresponding to $m_j \lesssim T_{\text{BH}}^{\text{in}}$, Eq. (3.22), and for large mass, when the time of allowed decay (when T_{BH} reaches m_j) is sufficiently short to avoid the overproduction of dark matter, Eq. (3.23). The allowed region widens for larger values of k . This is easily understandable by the fact that the memory burden effect extends the lifetime of PBH, diluting them further

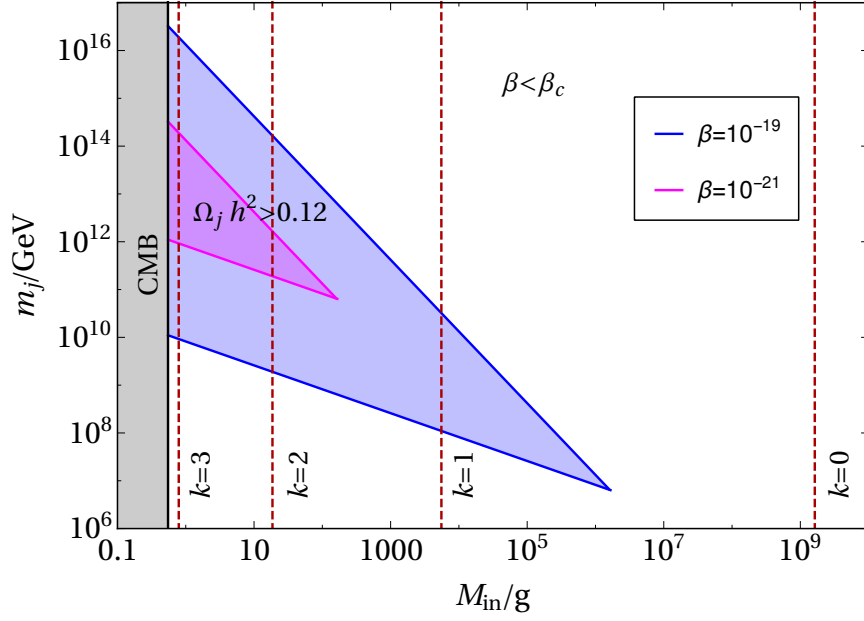


Figure 5. The values of the dark matter mass are plotted here as a function of the formation mass of PBHs for the case where the evaporation happens during radiation domination, i.e., $\beta < \beta_c$. The black lines represent the minimum mass possible for PBHs calculated considering the maximum energy scale of inflation. The vertical red dashed lines represent the maximum M_{in} values allowed to be consistent with the BBN bound. The shaded regions correspond to dark matter overproduction, $\Omega_j h^2 > 0.12$. We have chosen $q = 1/2$ and plotted two different values of $\beta = 10^{-19}$ and 10^{-21} , which are shown in blue and magenta, respectively.

and then decaying. More diluted black holes imply a more diluted dark matter production, which requires a larger mass m_j to fit with the relic abundance constraints. The effect is the opposite if one decreases q because, in this case, the memory burden effect is *delayed*, and a larger population of PBH decay follows the semiclassical approximation as we can see in Fig. 4 (right). In the limit $q \rightarrow 0$, we recover exactly the semiclassical limit. Moreover, Note that once $\beta > \beta_c$, the relic abundance no longer depends on β .

3.2.3 $\beta < \beta_c$

For $\beta < \beta_c$, PBHs evaporate during radiation domination, so there is no PBH domination. The Hubble parameter at the point of evaporation is then given by

$$H^2(a_{\text{ev}}) = \frac{\rho_R(a_{\text{ev}})}{3M_P^2} = \frac{g_* \pi^2 T_{\text{ev}}^4}{90M_P^2} = \frac{(\Gamma_{\text{BH}}^k)^2}{4}, \quad (3.24)$$

which gives the evaporation temperature

$$T_{\text{ev}} = M_P \left(\frac{3}{4\alpha} \right)^{1/4} \left[(3 + 2k) 2^k \epsilon \left(\frac{M_P}{q M_{\text{in}}} \right)^{3+2k} \right]^{1/2}. \quad (3.25)$$

During radiation dominated era, taking $H = 1/(2t)$ and $a \propto t^{1/2}$, using

$$n_{\text{BH}}(a_{\text{ev}}) = n_{\text{BH}}(a_{\text{in}}) \left(\frac{a_{\text{in}}}{a_{\text{ev}}} \right)^3 = \frac{\beta \rho_R^{\text{in}}}{M_{\text{in}}} \left(\frac{a_{\text{in}}}{a_{\text{ev}}} \right)^3, \quad \frac{a_{\text{in}}}{a_{\text{ev}}} = \sqrt{\frac{H(a_{\text{ev}})}{H_{\text{in}}}} = \sqrt{\frac{\Gamma_{\text{BH}}^k}{2H_{\text{in}}}}, \quad (3.26)$$

and H_{in} given by Eq. (2.4), we get the number density of the PBH to be

$$n_{\text{BH}}(a_{\text{ev}}) = 3 \beta M_P^3 \left(\frac{\pi \gamma}{2} \right)^{1/2} \left(\frac{(3+2k)2^k \epsilon}{q^{3+2k}} \right)^{3/2} \left(\frac{M_P}{M_{\text{in}}} \right)^{6+3k}. \quad (3.27)$$

Finally Combining Eq. (3.18) together with Eqs. (3.25) and (3.27), we have DM abundance today for $m_j < T_{\text{BH}}^{\text{in}}$

$$\frac{\Omega_j h^2}{0.12} = 2.54 \times 10^6 \beta \xi g_j \left(\frac{M_{\text{in}}}{M_P} \right)^{\frac{1}{2}} \frac{m_j}{\text{GeV}} \simeq \xi g_j \left(\frac{\beta}{10^{-20}} \right) \left(\frac{M_{\text{in}}}{1 \text{ g}} \right)^{\frac{1}{2}} \left(\frac{m_j}{8.2 \times 10^{10} \text{ GeV}} \right). \quad (3.28)$$

On the other hand, by doing the same analysis, one can arrive at the following expression for $m_j > T_{\text{BH}}^{\text{in}}$

$$\frac{\Omega_j h^2}{0.12} = 1.47 \times 10^{43} \beta \xi g_j \left(\frac{M_P}{M_{\text{in}}} \right)^{\frac{3}{2}} \frac{\text{GeV}}{m_j} \simeq \xi g_j \left(\frac{\beta}{10^{-20}} \right) \left(\frac{1 \text{ g}}{M_{\text{in}}} \right)^{\frac{3}{2}} \left(\frac{1.3 \times 10^{15} \text{ GeV}}{m_j} \right). \quad (3.29)$$

From the above expressions for two different cases Eqs. (3.28) and (3.29), it is interesting to note that the DM relic abundance is independent of the memory burden parameter k . This is easily understandable as, in this case, the total number of produced dark matter particles is the same irrespective of the physics behind the PBH decay, and further, the dilution effect is exclusively due to the radiation background.

We show in Fig. 5 the relic abundance constraint for $q = 1/2$ and two different values of $\beta = 10^{-19}$ and 10^{-21} , well below β_c as one can see from Fig. 3. We note that for the case $\beta < \beta_c$ the parameter space follows a triangular exclusion zone in the center limited by the cases $m_j < T_{\text{BH}}^{\text{in}}$ and $m_j > T_{\text{BH}}^{\text{in}}$. However, we indeed see that such shape of the constraints region does not depend on the burden parameter k anymore except for setting the maximum value M_{in} represented by red dashed lines. As stated earlier, this is due to the fact that the total number of dark matter particles produced is the same for both semiclassical and quantum-corrected PBH evaporation processes in conjunction with the radiation background. On the other hand, as expected, there exists a strong dependence of the relic density on β , for this parameter determines the relative amount of PBHs present in the thermal plasma, which will eventually decay (proportionally to β) into dark matter.

3.3 Dark matter from the stable PBHs with Hawking evaporation (*phase-I*) before BBN

Let us now look into the detail of the situation where standard Hawking evaporation takes place *before* BBN while the memory burden effect delays the complete evaporation, making the PBHs decay *after* the present time, rendering them stable on the cosmological scale. In this case, the total dark matter relic (Ω_{DM}) has two contributions: the dark matter as stable fundamental particles (Ω_j) produced from PBH evaporation computed in the previous sections *plus* the stable PBHs Ω_{PBH} that contribute also to the dark component of the Universe : $\Omega_{\text{DM}} = \Omega_j + \Omega_{\text{PBH}}$. This is attributed to the allowed region in white tagged as “Stable PBHs” in Fig. 2.

To compute the dark matter abundance generated by the evaporation during *phase-I*, Ω_j , we can use the expression for present-day DM relic due to evaporation, Eq. (3.18), taken at t_q , the time duration of *phase-I*:

$$\Omega_j h^2 = 1.6 \times 10^8 \frac{g_0}{g_q} \frac{n_j(a_q)}{T^3(a_q)} \frac{m_j}{\text{GeV}}, \quad (3.30)$$

where g_q is the effective number of degrees of freedom for the entropy at the end of *phase-I*, which we assume has the same value⁴ as g_{ev} . The ratio $n_j(a_q)/T^3(a_q)$ is given by⁵

$$\frac{n_j(a_q)}{T^3(a_q)} = N_j \frac{n_{\text{BH}}(a_{\text{in}})}{T_{\text{in}}^3} = N_j \frac{\beta \alpha T_{\text{in}}}{M_{\text{in}}}, \quad (3.31)$$

where T_{in} is the radiation temperature at the point of formation, and we supposed the Universe is radiation-dominated during the semiclassical phase ($\beta < \beta_c$). Following Eq. (2.4) we have

$$T_{\text{in}} = \left(\frac{48\pi^2 \gamma^2}{\alpha} \right)^{1/4} \sqrt{\frac{M_P}{M_{\text{in}}}} M_P, \quad (3.32)$$

Now, upon substitution of Eqs. (3.31) and (3.32) into (3.30), the final expression for DM relic from evaporation

$$\frac{\Omega_j h^2}{0.12} \simeq 1.5 \times 10^9 N_j \beta \left(\frac{M_P}{M_{\text{in}}} \right)^{3/2} \frac{m_j}{\text{GeV}}, \quad (3.33)$$

Where the total number of particles emitted per PBHs from *phase-I*, are given by Eqs. (3.6) and (3.9)

$$N_j = \frac{15 \xi g_j \zeta(3)}{g_*(T_{\text{BH}}) \pi^4} \begin{cases} (1 - q^2) \frac{M_{\text{in}}^2}{M_P^2}, & \text{for } m_j < T_{\text{BH}}^{\text{in}} \\ \frac{M_P^2}{m_j^2} - \frac{q^2 M_{\text{in}}^2}{M_P^2}, & \text{for } \frac{T_{\text{BH}}^{\text{in}}}{q} > m_j > T_{\text{BH}}^{\text{in}} \end{cases}. \quad (3.34)$$

We then need to consider the contribution from stable PBHs. Their relic abundance can be written as

$$\Omega_{\text{PBH}} h^2 = 1.6 \times 10^8 \frac{g_0}{g_q} \frac{\rho_{\text{BH}}(a_q)}{T^3(a_q)} \frac{1}{\text{GeV}}. \quad (3.35)$$

Connecting the end of *phase-I* with the formation point, one can find the ratio

$$\frac{\rho_{\text{BH}}(a_q)}{T^3(a_q)} = \frac{q \rho_{\text{BH}}(a_{\text{in}})}{T^3(a_{\text{in}})} = q \beta \alpha T_{\text{in}}, \quad (3.36)$$

where we assumed that the relativistic degrees of freedom associated with radiation at the point of formation and at the end of the semiclassical phase are the same. Finally, combining Eq. (3.32) with Eq. (3.36), and substituting into Eq. (3.35), we obtain the density of stable PBHs to be

$$\frac{\Omega_{\text{PBH}} h^2}{0.12} = 3.5 \times 10^{27} q \beta \left(\frac{M_P}{M_{\text{in}}} \right)^{1/2} \simeq q \left(\frac{\beta}{1.4 \times 10^{-25}} \right) \left(\frac{1 \text{ g}}{M_{\text{in}}} \right)^{1/2}. \quad (3.37)$$

⁴Generalization for any g_q is straightforward.

⁵We supposed here $\beta < \beta_c$ as when stable PBHs contribute to the entire dark matter, PBH domination starts roughly at the standard radiation-matter equality.

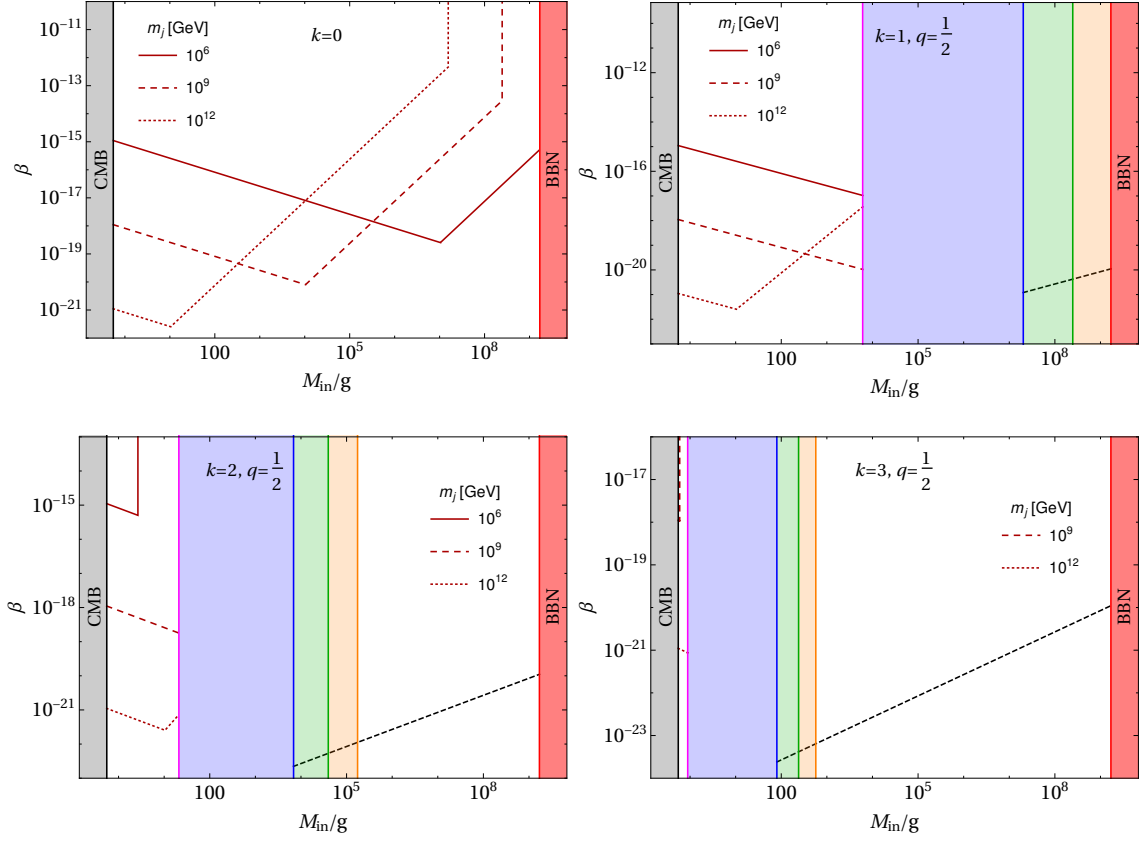


Figure 6. The critical values of β corresponding to the total dark matter density are plotted in brown as a function of PBH mass when the dark matter is emitted from the evaporation of PBHs before BBN. We have chosen three different values of dark matter mass, where $m_j = 10^6$ GeV, 10^9 GeV, and 10^{12} GeV are plotted in solid, dashed, and dotted lines, respectively. The black dashed lines correspond to the critical β when the stable PBHs contribute to the total dark matter energy density. The black-shaded region is excluded from the minimum PBH mass possible, corresponding to the highest energy scale of inflation. The red-shaded region indicates the PBH masses whose phase-I of evaporation ends after BBN. The blue regions correspond to the masses for which PBHs evaporate after BBN. The green and orange shaded regions are constraints coming from CMB and extragalactic γ -rays where $f_{\text{PBH}} < 1$.

Note that the quantity on the left side is also described as $f_{\text{PBH}} = \Omega_{\text{PBH}} h^2 / 0.12$, which is the fraction of total dark matter that comes from stable PBHs today. Finally, the total dark matter relic would be the sum of the contribution from evaporation in *phase-I*, Eq. (3.33) and from the stable PBHs which acts as dark matter, (3.37), which gives

$$\frac{\Omega_{\text{DM}} h^2}{0.12} = 3.5 \times 10^{27} \beta \left(\frac{M_P}{M_{\text{in}}} \right)^{1/2} \left[q + N_j \frac{m_j}{M_{\text{in}}} \right], \quad (3.38)$$

which is the key equation of our paper. It summarizes the amount of dark components due to stable PBH and its dark products. We expect domination of the dark products for small M_{in} , whereas PBH relics dominates for larger M_{in} .

Indeed, to summarize, we show for comparison in Fig. 6 the parameter space allowed by the relic abundance constraint in the plane (M_{in}, β) , in three cases : without taking into account the burden effect ($k = 0$), and with burden effect for $k = 1, 2$ and 3 for $q = 1/2$ and

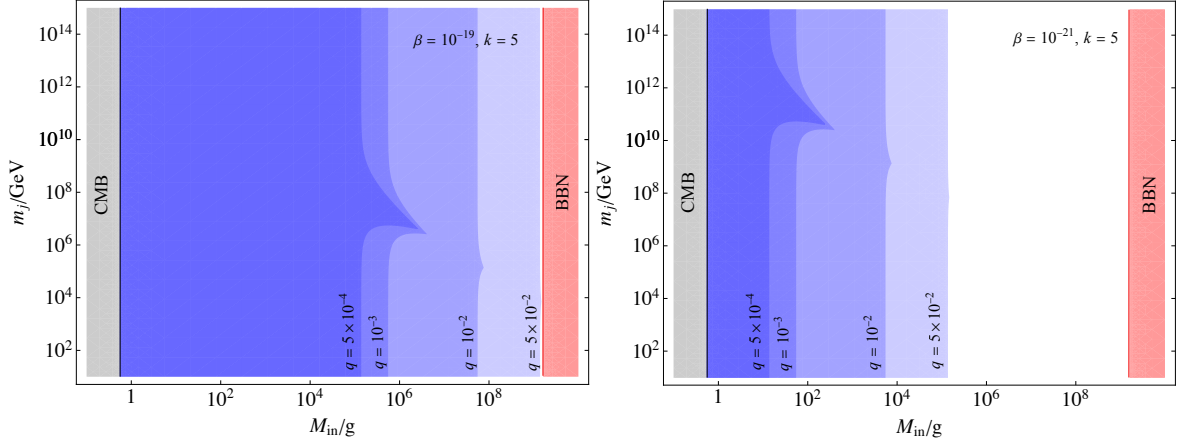


Figure 7. Dark matter mass as a function of the PBH mass taking into account the contribution from both the evaporation product and the stable PBHs. We have chosen two different values of β ($\beta = 10^{-19}$ -left and $\beta = 10^{-21}$ -right). In both cases, we shaded the excluded (overdense) region for four different values of q ($q = 5 \times 10^{-2}$, 10^{-2} , 10^{-3} and 5×10^{-4}). The grey-shaded region is excluded from the minimum PBH mass possible, corresponding to the highest energy scale of inflation. The red-shaded region indicates the PBH masses whose phase-I of evaporation ends after BBN. We see that for $q \gtrsim 10^{-2}$, the contributions to the total DM due to the evaporation are negligible compared to the contributions from the stable PBHs, see the text for detail.

$m_j = 10^6$, 10^9 and 10^{12} GeV. We first distinguish the two white regions, for low M_{in} and larger M_{in} , corresponding to the “Evaporate before BBN” and “Stable PBHs” of Fig. 2. For $k = 0$, in the mass range $1 \text{ g} \lesssim M_{\text{in}} \lesssim 10^9 \text{ g}$ the PBHs decay completely before BBN, and the correct relic abundance is accomplished, depicted by the brown lines by their decay product to a fundamental dark component in the first panel of Fig. 6. They follow the behavior $\beta \propto M_{\text{in}}^{-1/2}$, see Eq. (3.28) when $m_j < T_{\text{BH}}^{\text{in}}$ ($M_{\text{in}} < \frac{10^{13} \text{ GeV}}{m_j} \text{ g}$), and $\beta \propto M_{\text{in}}^{3/2}$, see Eq. (3.29) when $m_j > T_{\text{BH}}^{\text{in}}$ ($M_{\text{in}} > \frac{10^{13} \text{ GeV}}{m_j} \text{ g}$).

We recognize the same region for $k = 1$ but with a restricted mass range, and the restriction is due to longer PBHs lifetime attributed to the memory burden effect, rendering PBHs of mass $10^4 \text{ g} < M_{\text{in}} < 10^7 \text{ g}$ to decay after BBN and before the present time. In addition to that, the mass range from $10^7 \text{ g} < M_{\text{in}} < 10^9 \text{ g}$ are stable PBHs with the first phase before BBN but still restricted by the constraints from the extragalactic γ rays and CMB anisotropy shown in the orange and green shaded regions of Fig. 6. On the other hand, for $k = 2$, a new unconstrained PBH mass window opens for large mass within $10^5 \text{ g} < M_{\text{in}} < 10^9 \text{ g}$, which survives at present due to the quantum effect and populates as total DM component, while in the mass range $1 \text{ g} < M_{\text{in}} < 20 \text{ g}$, still keeping the possibility of the DM to be populated by the dark matter product from PBH decay. In the case of stable PBH, the relic abundance is given by $\beta \propto M_{\text{in}}^{1/2}$ as one can see from Eq. (3.37). Finally, only PBH as a dark matter is allowed for $k \geq 3$, with PBH relic densities not depending on k . This set of 4 figures nicely summarizes our work. Note that we set the q value at $1/2$ to do this analysis.

However, to complete our analysis, we also show the dependence on q in Fig. 7, for $\beta = 10^{-19}$ (left) and $\beta = 10^{-21}$ (right), corresponding to the values used in Fig. 5 for comparison. The shadowed region is excluded because it corresponds to parameter space, where there is an overproduction of dark matter. The limit $q = 0$ on the left region corresponds to the semiclassical approximation, i.e., the memory burden effect never occurs. This limit

corresponds to the situation where $\sim 100\%$ of the dark matter is composed of the decay products of PBH because there are no stable PBHs in this mass range. We can recognize the peak of the triangle shape of Fig. 5 appearing at $M_{\text{in}} \simeq 10^6 \text{ g}$ ($\simeq 100 \text{ g}$) for $\beta = 10^{-19}$ ($\beta = 10^{-21}$). For larger value of q , we know from Fig. 6 that for $\beta = 10^{-19}$, PBH cannot be a dark matter candidate, as they would overpopulate the Universe. That explains why all the regions are shadowed in Fig. 7 left. However, for $\beta = 10^{-21}$, we can evaluate from Fig. 6 bottom-left that M_{in} should be larger than $\sim 10^7 \text{ g}$ for $q = 1/2$. But we see from Fig. 7 right that a larger region is allowed, up to the range $10 \text{ g} \lesssim M_{\text{in}} \lesssim 10^9 \text{ g}$ for $q = 5 \times 10^{-4}$. Indeed, for a fixed β value, smaller values of q induce a latter burden effect, and a smaller stable PBH mass is required to satisfy the total DM relic. In summary, for stable PBHs with q values $q \leq 10^{-2}$, there is a possibility that DM from PBH decay also contributes to the total DM relic, depending on the mass of the DM. However, for higher q values $q \geq 10^{-2}$, the dark matter from stable PBHs always dominates over the decay products.

4 Conclusions

We computed the relic abundance in the presence of PBH beyond the semiclassical approximation. Indeed, when the mass of a BH reaches a certain fraction q of its initial value, the backreaction can not be ignored, and it can potentially reduce the evaporation rate by the inverse power law of its entropy S^{-k} . Taking into account this effect due to the memory burden effect, we added the dark component produced by the decay of PBHs during the early stage to the contribution of stable PBHs whose lifetime is extended due to the quantum corrections. Since the lifetime of the BH is extended depending on the memory burden parameters k and q , for the scenario of PBH domination, the duration of the PBH domination is also extended. As a result, the allowed region in m_j versus M_{in} parameter space is extended as we increase k for a fixed q or increase q for a fixed k ; that is also reflected in Fig. 4. Whereas, in the case of PBH decay in a background dominated by radiation, the memory burden parameters limit the highest permitted BH mass that completes the decay process before BBN and has no effect on the dark matter mass range, which we can see in Fig. 5. Depending on the strength of the burden effect, we show that PBH decay products can satisfy the relic density constraints for PBH masses below $\lesssim (6 \times 10^3, 20, 1) \text{ g}$ for $k = (1, 2, 3)$, respectively. Moreover, with an increase in $k > 3$, there is no DM parameter space from PBH decay. Note that all of these mentioned values are quoted for considering *phase - I* being complete after half-life, $q = 1/2$. On the other hand, PBH mass in the range $10^3 - 10^9 \text{ g}$ can be sufficiently stable and numerous to fulfill the relic abundance of DM for $k = 3$. The range of allowed masses even extends to $1 \text{ g} - 10^9 \text{ g}$ for $k \geq 5$, see Fig. 2. We also show that decreasing the value of q down to $\sim 10^{-2}$ reopens the dark matter parameter space from PBH decay, then we need to consider the contribution from both PBH decay and stable PBHs. Our results are thus nicely summarized in Figs. 2, 6 and 7, with Eq. (3.38).

Acknowledgments

The authors want to warmly thank Donald Kpatcha, Simon Clery, Mathieu Gross, and Lucien Heurtier for extremely useful discussions during the Astro@Paris-Saclay symposium 2023. This project has received support from the European Union's Horizon 2020 research and innovation program under the Marie Skłodowska-Curie grant agreement No 860881-HIDDeN and the CNRS-IRP project UCMN. MRH wishes to acknowledge support from the

Science and Engineering Research Board (SERB), Government of India (GoI), for the SERB National Post-Doctoral fellowship, File Number: PDF/2022/002988. SM wishes to thank the Indian Institute of Technology (IIT) Madras, Chennai, India, for support through the Exploratory Research Project RF22230527PHRFER008479. SM also wishes to acknowledge the support from project SB22231259PHETWO008479 for the travel grant for Astro@Paris-Saclay symposium 2023. DM wishes to acknowledge support from the Science and Engineering Research Board (SERB), Department of Science and Technology (DST), Government of India (GoI), through the Core Research Grant CRG/2020/003664.

References

- [1] B. J. Carr and S. W. Hawking, *Black holes in the early Universe*, *Mon. Not. Roy. Astron. Soc.* **168** (1974) 399–415.
- [2] S. Hawking, *Gravitationally collapsed objects of very low mass*, *Mon. Not. Roy. Astron. Soc.* **152** (1971) 75.
- [3] B. J. Carr and S. W. Hawking, *Black Holes in the Early Universe*, *Monthly Notices of the Royal Astronomical Society* **168** (08, 1974) 399–415, [<https://academic.oup.com/mnras/article-pdf/168/2/399/8079885/mnras168-0399.pdf>].
- [4] P. Ivanov, P. Naselsky, and I. Novikov, *Inflation and primordial black holes as dark matter*, *Phys. Rev. D* **50** (1994) 7173–7178.
- [5] N. Bartolo, V. De Luca, G. Franciolini, A. Lewis, M. Peloso, and A. Riotto, *Primordial Black Hole Dark Matter: LISA Serendipity*, *Phys. Rev. Lett.* **122** (2019), no. 21 211301, [[arXiv:1810.12218](https://arxiv.org/abs/1810.12218)].
- [6] B. Carr and F. Kuhnel, *Primordial Black Holes as Dark Matter: Recent Developments*, *Ann. Rev. Nucl. Part. Sci.* **70** (2020) 355–394, [[arXiv:2006.02838](https://arxiv.org/abs/2006.02838)].
- [7] K. Jedamzik, *Primordial Black Hole Dark Matter and the LIGO/Virgo observations*, *JCAP* **09** (2020) 022, [[arXiv:2006.11172](https://arxiv.org/abs/2006.11172)].
- [8] K. Jedamzik, *Consistency of Primordial Black Hole Dark Matter with LIGO/Virgo Merger Rates*, *Phys. Rev. Lett.* **126** (2021), no. 5 051302, [[arXiv:2007.03565](https://arxiv.org/abs/2007.03565)].
- [9] A. M. Green and B. J. Kavanagh, *Primordial Black Holes as a dark matter candidate*, *J. Phys. G* **48** (2021), no. 4 043001, [[arXiv:2007.10722](https://arxiv.org/abs/2007.10722)].
- [10] P. Villanueva-Domingo, O. Mena, and S. Palomares-Ruiz, *A brief review on primordial black holes as dark matter*, *Front. Astron. Space Sci.* **8** (2021) 87, [[arXiv:2103.12087](https://arxiv.org/abs/2103.12087)].
- [11] B. Carr and F. Kuhnel, *Primordial black holes as dark matter candidates*, *SciPost Phys. Lect. Notes* **48** (2022) 1, [[arXiv:2110.02821](https://arxiv.org/abs/2110.02821)].
- [12] D. Baumann, P. J. Steinhardt, K. Takahashi, and K. Ichiki, *Gravitational Wave Spectrum Induced by Primordial Scalar Perturbations*, *Phys. Rev. D* **76** (2007) 084019, [[hep-th/0703290](https://arxiv.org/abs/hep-th/0703290)].
- [13] J. R. Espinosa, D. Racco, and A. Riotto, *A Cosmological Signature of the SM Higgs Instability: Gravitational Waves*, *JCAP* **09** (2018) 012, [[arXiv:1804.07732](https://arxiv.org/abs/1804.07732)].
- [14] G. Domènech, *Induced gravitational waves in a general cosmological background*, *Int. J. Mod. Phys. D* **29** (2020), no. 03 2050028, [[arXiv:1912.05583](https://arxiv.org/abs/1912.05583)].
- [15] H. V. Ragavendra, P. Saha, L. Sriramkumar, and J. Silk, *Primordial black holes and secondary gravitational waves from ultraslow roll and punctuated inflation*, *Phys. Rev. D* **103** (2021), no. 8 083510, [[arXiv:2008.12202](https://arxiv.org/abs/2008.12202)].
- [16] K. Inomata, K. Kohri, and T. Terada, *The Detected Stochastic Gravitational Waves and Subsolar-Mass Primordial Black Holes*, [[arXiv:2306.17834](https://arxiv.org/abs/2306.17834)].

- [17] G. Franciolini, A. Iovino, Junior., V. Vaskonen, and H. Veermae, *The recent gravitational wave observation by pulsar timing arrays and primordial black holes: the importance of non-gaussianities*, [arXiv:2306.17149](#).
- [18] H. Firouzjahi and A. Talebian, *Induced Gravitational Waves from Ultra Slow-Roll Inflation and Pulsar Timing Arrays Observations*, [arXiv:2307.03164](#).
- [19] S. Maity, N. Bhaumik, M. R. Haque, D. Maity, and L. Sriramkumar, *Constraining the history of reheating with the NANOGrav 15-year data*, [arXiv:2403.16963](#).
- [20] S. W. Hawking, *Black hole explosions*, *Nature* **248** (1974) 30–31.
- [21] S. W. Hawking, *Particle Creation by Black Holes*, *Commun. Math. Phys.* **43** (1975) 199–220. [Erratum: *Commun.Math.Phys.* 46, 206 (1976)].
- [22] M. Riajul Haque, E. Kpatcha, D. Maity, and Y. Mambrini, *Primordial black hole reheating*, *Phys. Rev. D* **108** (2023), no. 6 063523, [[arXiv:2305.10518](#)].
- [23] N. Bernal, C. S. Fong, Y. F. Perez-Gonzalez, and J. Turner, *Rescuing high-scale leptogenesis using primordial black holes*, *Phys. Rev. D* **106** (2022), no. 3 035019, [[arXiv:2203.08823](#)].
- [24] B. Barman, S. Jyoti Das, M. R. Haque, and Y. Mambrini, *A Gravitational Ménage à Trois: leptogenesis, primordial gravitational wave & PBH-induced reheating*, [arXiv:2403.05626](#).
- [25] R. Calabrese, M. Chianese, J. Gunn, G. Miele, S. Morisi, and N. Saviano, *Limits on light primordial black holes from high-scale leptogenesis*, *Phys. Rev. D* **107** (2023), no. 12 123537, [[arXiv:2305.13369](#)].
- [26] S. Sugiyama, V. Takhistov, E. Vitagliano, A. Kusenko, M. Sasaki, and M. Takada, *Testing Stochastic Gravitational Wave Signals from Primordial Black Holes with Optical Telescopes*, *Phys. Lett. B* **814** (2021) 136097, [[arXiv:2010.02189](#)].
- [27] K. Inomata, M. Kawasaki, K. Mukaida, T. Terada, and T. T. Yanagida, *Gravitational Wave Production right after a Primordial Black Hole Evaporation*, *Phys. Rev. D* **101** (2020), no. 12 123533, [[arXiv:2003.10455](#)].
- [28] G. Domènech, C. Lin, and M. Sasaki, *Gravitational wave constraints on the primordial black hole dominated early universe*, *JCAP* **04** (2021) 062, [[arXiv:2012.08151](#)]. [Erratum: *JCAP* 11, E01 (2021)].
- [29] G. Domènech, V. Takhistov, and M. Sasaki, *Exploring evaporating primordial black holes with gravitational waves*, *Phys. Lett. B* **823** (2021) 136722, [[arXiv:2105.06816](#)].
- [30] N. Bhaumik, A. Ghoshal, and M. Lewicki, *Doubly peaked induced stochastic gravitational wave background: testing baryogenesis from primordial black holes*, *JHEP* **07** (2022) 130, [[arXiv:2205.06260](#)].
- [31] N. Bhaumik, A. Ghoshal, R. K. Jain, and M. Lewicki, *Distinct signatures of spinning PBH domination and evaporation: doubly peaked gravitational waves, dark relics and CMB complementarity*, *JHEP* **05** (2023) 169, [[arXiv:2212.00775](#)].
- [32] A. Ghoshal, Y. Gouttenoire, L. Heurtier, and P. Simakachorn, *Primordial black hole archaeology with gravitational waves from cosmic strings*, *JHEP* **08** (2023) 196, [[arXiv:2304.04793](#)].
- [33] S. Balaji, G. Domènech, G. Franciolini, A. Ganz, and J. Tränkle, *Probing modified Hawking evaporation with gravitational waves from the primordial black hole dominated universe*, [arXiv:2403.14309](#).
- [34] A. Cheek, L. Heurtier, Y. F. Perez-Gonzalez, and J. Turner, *Primordial black hole evaporation and dark matter production. I. Solely Hawking radiation*, *Phys. Rev. D* **105** (2022), no. 1 015022, [[arXiv:2107.00013](#)].
- [35] M. R. Haque, E. Kpatcha, D. Maity, and Y. Mambrini, *Primordial black hole versus inflaton*, *Phys. Rev. D* **109** (2024), no. 2 023521.

- [36] A. Cheek, L. Heurtier, Y. F. Perez-Gonzalez, and J. Turner, *Primordial black hole evaporation and dark matter production. II. Interplay with the freeze-in or freeze-out mechanism*, *Phys. Rev. D* **105** (2022), no. 1 015023, [[arXiv:2107.00016](#)].
- [37] N. Bernal, Y. F. Perez-Gonzalez, and Y. Xu, *Superradiant production of heavy dark matter from primordial black holes*, *Phys. Rev. D* **106** (2022), no. 1 015020, [[arXiv:2205.11522](#)].
- [38] D. N. Page and S. W. Hawking, *Gamma rays from primordial black holes*, *Astrophys. J.* **206** (1976) 1–7.
- [39] J. H. MacGibbon and B. J. Carr, *Cosmic rays from primordial black holes*, *Astrophys. J.* **371** (1991) 447–469.
- [40] G. Ballesteros, J. Coronado-Blázquez, and D. Gaggero, *X-ray and gamma-ray limits on the primordial black hole abundance from hawking radiation*, *Physics Letters B* **808** (2020) 135624.
- [41] K. Kohri and J. Yokoyama, *Primordial black holes and primordial nucleosynthesis: Effects of hadron injection from low mass holes*, *Phys. Rev. D* **61** (Dec, 1999) 023501.
- [42] B. J. Carr, K. Kohri, Y. Sendouda, and J. Yokoyama, *New cosmological constraints on primordial black holes*, *Phys. Rev. D* **81** (2010) 104019, [[arXiv:0912.5297](#)].
- [43] V. Poulin, J. Lesgourgues, and P. D. Serpico, *Cosmological constraints on exotic injection of electromagnetic energy*, *JCAP* **03** (2017) 043, [[arXiv:1610.10051](#)].
- [44] S. Clark, B. Dutta, Y. Gao, L. E. Strigari, and S. Watson, *Planck Constraint on Relic Primordial Black Holes*, *Phys. Rev. D* **95** (2017), no. 8 083006, [[arXiv:1612.07738](#)].
- [45] H. Niikura et al., *Microlensing constraints on primordial black holes with Subaru/HSC Andromeda observations*, *Nature Astron.* **3** (2019), no. 6 524–534, [[arXiv:1701.02151](#)].
- [46] D. Croon, D. McKeen, N. Raj, and Z. Wang, *Subaru-HSC through a different lens: Microlensing by extended dark matter structures*, *Phys. Rev. D* **102** (2020), no. 8 083021, [[arXiv:2007.12697](#)].
- [47] K. Griest, A. M. Cieplak, and M. J. Lehner, *Experimental Limits on Primordial Black Hole Dark Matter from the First 2 yr of Kepler Data*, *Astrophys. J.* **786** (2014), no. 2 158, [[arXiv:1307.5798](#)].
- [48] B. Carr, K. Kohri, Y. Sendouda, and J. Yokoyama, *Constraints on primordial black holes*, *Rept. Prog. Phys.* **84** (2021), no. 11 116902, [[arXiv:2002.12778](#)].
- [49] G. Dvali and C. Gomez, *Black Holes as Critical Point of Quantum Phase Transition*, *Eur. Phys. J. C* **74** (2014) 2752, [[arXiv:1207.4059](#)].
- [50] G. Dvali, L. Eisemann, M. Michel, and S. Zell, *Black hole metamorphosis and stabilization by memory burden*, *Phys. Rev. D* **102** (2020), no. 10 103523, [[arXiv:2006.00011](#)].
- [51] A. Alexandre, G. Dvali, and E. Koutsangelas, *New Mass Window for Primordial Black Holes as Dark Matter from Memory Burden Effect*, [[arXiv:2402.14069](#)].
- [52] V. Thoss, A. Burkert, and K. Kohri, *Breakdown of Hawking Evaporation opens new Mass Window for Primordial Black Holes as Dark Matter Candidate*, [[arXiv:2402.17823](#)].
- [53] P. Ivanov, P. Naselsky, and I. Novikov, *Inflation and primordial black holes as dark matter*, *Phys. Rev. D* **50** (Dec, 1994) 7173–7178.
- [54] J. Yokoyama, *Chaotic new inflation and formation of primordial black holes*, *Phys. Rev. D* **58** (1998) 083510, [[astro-ph/9802357](#)].
- [55] K. Kohri, D. H. Lyth, and A. Melchiorri, *Black hole formation and slow-roll inflation*, *JCAP* **04** (2008) 038, [[arXiv:0711.5006](#)].
- [56] T. Harada, C.-M. Yoo, and K. Kohri, *Threshold of primordial black hole formation*, *Phys. Rev. D* **88** (2013), no. 8 084051, [[arXiv:1309.4201](#)]. [Erratum: *Phys.Rev.D* 89, 029903 (2014)].

- [57] S. Bhattacharya, S. Mohanty, and P. Parashari, *Primordial black holes and gravitational waves in nonstandard cosmologies*, *Phys. Rev. D* **102** (2020), no. 4 043522, [[arXiv:1912.01653](#)].
- [58] S. W. Hawking, I. G. Moss, and J. M. Stewart, *Bubble Collisions in the Very Early Universe*, *Phys. Rev. D* **26** (1982) 2681.
- [59] S. G. Rubin, A. S. Sakharov, and M. Y. Khlopov, *The Formation of primary galactic nuclei during phase transitions in the early universe*, *J. Exp. Theor. Phys.* **91** (2001) 921–929, [[hep-ph/0106187](#)].
- [60] V. Dokuchaev, Y. Eroshenko, and S. Rubin, *Quasars formation around clusters of primordial black holes*, *Grav. Cosmol.* **11** (2005) 99–104, [[astro-ph/0412418](#)].
- [61] C. J. Hogan, *Massive black holes generated by cosmic strings*, *Physics Letters B* **143** (1984), no. 1 87–91.
- [62] S. Hawking, *Black holes from cosmic strings*, *Physics Letters B* **231** (1989), no. 3 237–239.
- [63] S. J. Huber, T. Konstandin, G. Nardini, and I. Rues, *Detectable Gravitational Waves from Very Strong Phase Transitions in the General NMSSM*, *JCAP* **03** (2016) 036, [[arXiv:1512.06357](#)].
- [64] C. Caprini et al., *Science with the space-based interferometer eLISA. II: Gravitational waves from cosmological phase transitions*, *JCAP* **04** (2016) 001, [[arXiv:1512.06239](#)].
- [65] P. S. B. Dev and A. Mazumdar, *Probing the Scale of New Physics by Advanced LIGO/VIRGO*, *Phys. Rev. D* **93** (2016), no. 10 104001, [[arXiv:1602.04203](#)].
- [66] D. G. Figueroa, M. Hindmarsh, and J. Urrestilla, *Exact Scale-Invariant Background of Gravitational Waves from Cosmic Defects*, *Phys. Rev. Lett.* **110** (2013), no. 10 101302, [[arXiv:1212.5458](#)].
- [67] S. A. Sanidas, R. A. Battye, and B. W. Stappers, *Constraints on cosmic string tension imposed by the limit on the stochastic gravitational wave background from the European Pulsar Timing Array*, *Phys. Rev. D* **85** (2012) 122003, [[arXiv:1201.2419](#)].
- [68] J. Auffinger, I. Masina, and G. Orlando, *Bounds on warm dark matter from Schwarzschild primordial black holes*, *Eur. Phys. J. Plus* **136** (2021), no. 2 261, [[arXiv:2012.09867](#)].
- [69] I. Masina, *Dark Matter and Dark Radiation from Evaporating Kerr Primordial Black Holes*, *Grav. Cosmol.* **27** (2021), no. 4 315–330, [[arXiv:2103.13825](#)].
- [70] J. H. MacGibbon and B. R. Webber, *Quark and gluon jet emission from primordial black holes: The instantaneous spectra*, *Phys. Rev. D* **41** (1990) 3052–3079.
- [71] **BICEP, Keck** Collaboration, P. A. R. Ade et al., *Improved Constraints on Primordial Gravitational Waves using Planck, WMAP, and BICEP/Keck Observations through the 2018 Observing Season*, *Phys. Rev. Lett.* **127** (2021), no. 15 151301, [[arXiv:2110.00483](#)].
- [72] **Planck** Collaboration, Y. Akrami et al., *Planck 2018 results. X. Constraints on inflation*, *Astron. Astrophys.* **641** (2020) A10, [[arXiv:1807.06211](#)].
- [73] Y. Mambrini, *Particles in the dark Universe*, Springer Ed., ISBN 978-3-030-78139-2 (2021).